Left Ventricular Ejection Fraction Assessed from Gated Technetium-99m-Sestamibi SPECT

E. Gordon DePuey, Kenneth Nichols and Cindy Dobrinsky

Division of Nuclear Medicine, Department of Radiology and Division of Cardiology, Department of Medicine, St. Luke's-Roosevelt Hospital Center and Columbia University College of Physicians and Surgeons, New York, New York

By means of ECG gating of tomographic (SPECT) ^{99m}Tc-sestamibi (MIBI) images, myocardial perfusion and wall thickening have been evaluated after a single tracer injection. To determine if left ventricular ejection fraction (LVEF) can also be measured from gated MIBI SPECT, 30 patients 1 wk to 6 mo after myocardial infarction (MI) received 22–30 mCi ^{99m}Tc-MIBI during treadmill exercise. Eight frame per cardiac cycle gated MIBI 180° SPECT was performed 60 min thereafter. Using 6.4-mm thick mid-ventricular vertical and horizontal long-axis slices from R-wave triggered end-diastolic and end-systolic frames, two independent observers manually drew endocardial borders at a count level of 34% of the maximum. LVEF was computed by the Simpson's rule method, corrected for the average point spread function of the SPECT camera. Results were correlated with LVEF determined from planar gated ^{99m}Tc-blood-pool studies performed within 4 days. LVEFs calculated from gated MIBI SPECT ranged from 0.21 to 0.73 and correlated linearly with gated blood-pool values (correlation coefficients ranged from 0.79 to 0.88; interobserver variability r = 0.75; intraobserver reproducibility r = 0.75). We conclude that in patients with MI resting LVEF can be determined from gated MIBI SPECT, thereby considerably augmenting the technique's diagnostic and prognostic value.

J Nucl Med 1993; 34:1871–1876

Technetium-99m-sestamibi (MIBI) perfusion imaging allows characterization of the extent and severity of perfusion abnormalities. The technique has been proven to size myocardial infarcts accurately (*1,2*), and some recent studies suggest that gated MIBI tomograms may provide better agreement with clinical findings of subtle perfusion abnormalities than do nongated tomograms (*3*). Electrocardiographic gating of MIBI SPECT images provides the additional ability to determine the severity of abnormalities in wall motion and wall thickening associated with myocardial infarcts (*4–5*). Since it is well recognized that prognosis in patients with myocardial infarction is inversely related to ejection fraction (EF), we investigated the feasibility of calculating resting left ventricular ejection fraction (LVEF) from gated MIBI SPECT images (*6–8*). Such quantitative assessment of ventricular function may augment the clinical value of perfusion imaging, and because we anticipate this to be of most value for patients who have suffered myocardial infarcts, we confined our attention to that patient group in this investigation.

Based upon data obtained from cardiac phantom studies, we developed a method whereby LVEF in patients was derived from end-diastolic (ED) and end-systolic (ES) endocardial borders of gated ^{99m}Tc-MIBI SPECT myocardial perfusion images. To validate the method, results were compared to LVEF values determined from conventional planar equilibrium radionuclide ventriculography.

METHODS

Patients

Thirty patients who had sustained documented myocardial infarction 1 wk to 6 mo previously were studied. There were 23 men and 7 women, ranging in age from 42 to 82 yr. Myocardial infarcts were documented by the presence of electrocardiographic Q-waves and/or cardiac enzyme elevation. Only the stress (exercise or intravenous dipyridamole) MIBI SPECT study was gated and used for LVEF determination. However, since the patient is at rest during image acquisition, performed 30–60 min after stress, resting wall motion is observed in images demonstrating perfusion at stress.

Equilibrium Radionuclide Angiocardiography

All patients underwent planar equilibrium radionuclide angiocardiography within 48 hr of gated ^{99m}Tc-sestamibi SPECT. Red blood cell labeling was performed using the in vivo method.

Patients received 2–3 mg stannous pyrophosphate intravenously followed 20 min later with an intravenous dose of 25 mCi ^{99m}Tc-pertechnetate. A commercially available General Electric XCT camera equipped with an all-purpose, parallel-hole collimator interfaced to a General Electric 3000 computer was used for all equilibrium studies. Thirty-two frames per cardiac cycle gated images were obtained in the "best septal" left anterior oblique (LAO), anterior and left lateral views. The LAO study, from which EF was determined, contained a total of five million counts. LVEF was calculated using a standard, commercially available, semiautomated technique (General Electric, Milwaukee, WI, SAGE software). An approximate region of interest (ROI) around the left ventricle (LV) was selected by the operator. By using

Received Dec. 17, 1992; revision accepted Jun. 23, 1993.

For correspondence or reprints contact: E. Gordon DePuey, MD, Division of Nuclear Medicine, St. Luke's-Roosevelt Hospital Center, Amsterdam Ave at 114th St., New York, NY 10025.

automated analysis, LV edges are then determined using a hybrid first and second derivative method. All edges were visually inspected for accuracy. LVEF was then calculated by a standard count rate based, background-corrected formula.

Gated Sestamibi SPECT

Stress and rest ^{99m}Tc-MIBI SPECT images were acquired in each patient using the same gamma camera and computer system described above for the gated blood-pool studies, except that a low-energy, high-resolution, parallel-hole collimator was employed rather than a general-purpose collimator. However, since for the purposes of the present study only the stress images were analyzed, the acquisition and processing of only the stress images is described below.

Technetium-99m-MIBI was injected either during peak treadmill exercise or 3 min following intravenous dipyridamole infusion (0.142 mg/kg/min administered over 4 min). These studies were the stress portions of either a separate-day or one-day rest/stress imaging protocol. For patients imaged with the one-day protocol, the average stress ^{99m}Tc-MIBI dose was 30 mCi. For patients studied using the separate-day protocol, the stress MIBI dose averaged 22 mCi. Sixty-four projection images were obtained as 64 × 64 matrices using a step-and-shoot acquisition over a 180° arc extending from the 45° right anterior oblique to 45° left posterior oblique position. Images were acquired for 20 sec per projection for a total imaging time of 25 min. Images were gated at eight frames per cardiac cycle using an R-wave trigger. Average (±1 s.d.) heart rate was 80 ± 14 bpm for the equilibrium radionuclide ventriculography studies and 84 ± 15 bpm for the gated sestamibi SPECT studies ($p = 0.08$).

Data Processing

Once a complete set of gated tomographic data was collected, it was possible to postprocess it in many different ways. First, all gated tomograms were added at each projection angle to produce a summed tomographic data set similar to that which would have been acquired without gating. Summed tomograms were reconstructed into transaxial slices. On the transaxial slice which exhibited the largest LV cavity (greatest mid-ventricular diameter), a line was drawn to bisect the LV, from which was formed the mid-ventricular vertical long-axis (VLA) slice, and on this image a line was again drawn bisecting the LV, from which the mid-ventricular horizontal long-axis (HLA) slice was generated. At these locations in the heart, the complete gated tomographic data set was used to construct eight frames per cardiac cycle of dynamic HLA and VLA tomograms. On the computer display, the HLA slices are automatically oriented vertically. The VLA images, which usually have a physiologic caudal tilt, were realigned to be as nearly horizontal as possible, as was necessary to provide the independent horizontal and vertical ventricular dimensions along orthogonal axes for proper input to Equations 1 and 3 below.

The gated MIBI images were prefiltered using a Hanning filter with a cutoff frequency of 0.7. During backprojection, a ramp filter was employed. Interslice spatial averaging was accomplished by adding adjacent frames in a staggered fashion [slice 1 + 2, 2 + 3, 3 + 4, . . . , (n − 1) + n]. Thus, each gated slice was two pixels in thickness (12.8 mm). Within each eight-frame data set, temporal filtering was used.

All eight HLA images were then displayed on the computer in both black and white and color simultaneously in both static format and in endless cinematic loop format. An observer identified the ED frame, which was then magnified by a factor of 4 and redisplayed beside a similarly magnified depiction of the HLA cine images. In all cases, the ED frame was verified to be frame #1. The observer then drew what he perceived to be the endocardial ED outline with a computer cursor. This process was repeated for drawing the ES outline on the selected HLA ES frame. In a similar manner, ED and ES endocardial outlines for the VLA images were drawn.

As already described, images were presented in a variety of formats as aids to the observers in deciding where to draw endocardial borders. These aids were especially important when defining borders of hypoperfused myocardium, for which observers were encouraged to freely alter brightness and contrast while previewing the images. For instance, Figure 1 demonstrates the end-diastolic VLA image for a post-MI patient, in which the color image does not define the inferior wall and endocardial border nearly as well as the black and white image due to the complete contrast range preserved in the lower third of the monochromatic scale. However, for consistency, once observers finished previewing data, the standardized color map shown on Figure 1 was used with the image brightness normalized automatically to the myocardial pixel with the maximum count.

LV endocardial border tracing and valve plane estimation from the gated MIBI studies was performed by two independent observers designated as observer 1 and observer 2. In addition, observer 2 performed the determination on two separate occasions 1 mo apart.

Volumetric Calculations

One method of approximating the volume of the left ventricular cavity is to compute it by assuming that each short-axis slice is an ellipsoidal solid and dividing the volume into slices of equal thickness "T" corresponding to the digitization dimension (6.4 cm/pixel) (Fig. 2). All short-axis slices can be sampled simultaneously by viewing the orthogonal VLA and HLA images. Labeling each of the short-axis slices by index j, starting from the first slice at the apex for $j = 1$ and proceeding to the last slice at the base for $j = N$, the vertical extent of each ellipsoid would be V_j and would be the number of pixels measured from the anterior endocardial border to the inferior endocardial border on the VLA image. The horizontal extent of the same ellipsoidal slice would be the number of pixels, H_j, between septal and lateral endocardial borders of the HLA image. The total ventricular volume would then be the sum of the volumes of the individual ellipsoidal cylinders.

Volume was then calculated using the elliptical version of Simpson's rule and the following formula, in which the volumes of the elliptical cylindrical slices were summed from the LV apex to the base for N slices:

$$V = \sum_{j=1}^{N} (\pi/4) H_j \times V_j \times T. \qquad \text{Eq. 1}$$

From end-diastolic volume (EDV) and end-systolic volume (ESV), LVEF was calculated:

$$LVEF = \frac{EDV - ESV}{EDV}. \qquad \text{Eq. 2}$$

In Figure 3, a representative normal patient study, the ED endocardial borders of the LV have been traced by the operator for the mid-ventricular vertical long-axis and horizontal long-axis slice.

In a preliminary examination of gated HLA and VLA images of

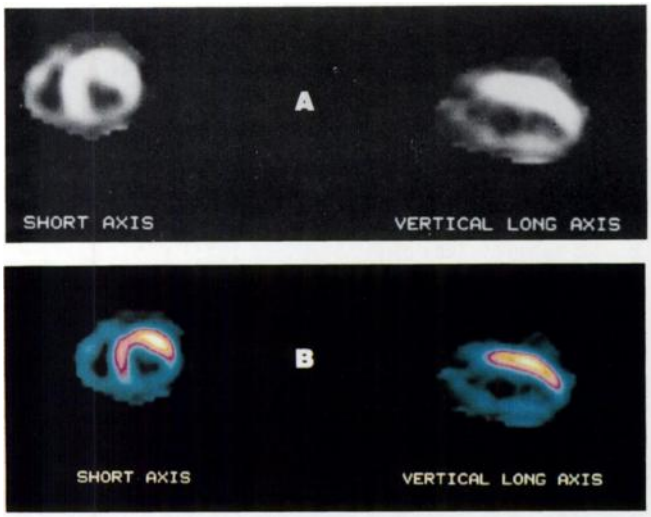

FIGURE 1. An example of a hypoperfused inferior myocardial wall seen better in the black and white display (A) than in the color display (B) of end-diastolic short-axis and vertical long-axis tomographic slices.

normal MIBI studies, observers perceived the endocardial borders as being at the sixth of 16 gray scales or color scales, with the 16th display level assigned to the highest counts. Thus, since the sixth level encompasses all counts between 31.25%–37.50% of the maximum, we concluded that our observers were most comfortable identifying endocardial borders of MIBI studies at an average of 34% of the maximum counts. Having established this guideline, subsequent observers were advised to draw their endocardial borders at this sixth level, which for the particular color table shown in Figure 3 occurred at the abrupt transition from magenta to blue. Note that the apex of the LV cavity is more easily defined than the base. The valve plane, or basal limit of the LV cavity, was defined as a straight line extending from the base of the septum to the base of the posterolateral wall.

Phantom Studies

It is well known that the finite resolution (on the order of 1–2 cm^3) of a gamma camera inevitably produces partial volume effects (*9*), resulting in errors in the identification of the position of endocardial and epicardial borders (*10*). Scattered radiation results in significant overestimation of myocardial wall thickness (*11*). Therefore, observers systematically underestimate left ventricular cavity dimensions when viewing tomographic myocardial perfusion scans.

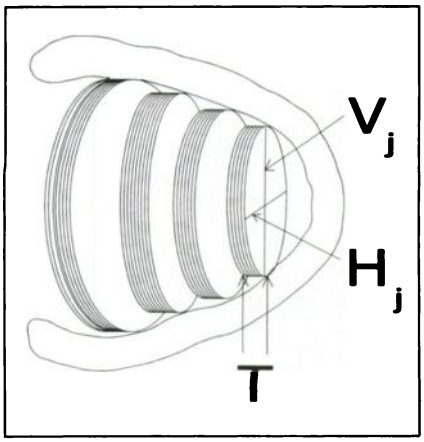

FIGURE 2. The left ventricular cavity may be considered a stack of elliptical cylinders with height V_j, width H and thickness T.

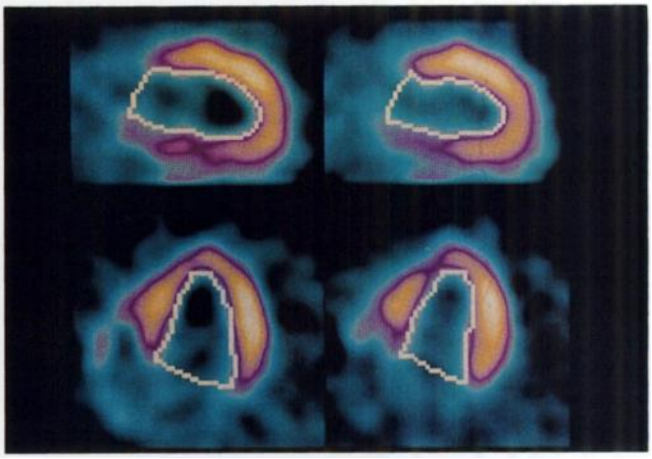

FIGURE 3. Mid-ventricular end-diastolic (left) and end-systolic (right) vertical long-axis (top) and horizontal long-axis (bottom) tomographic slices. The manually determined endocardial borders and valve plane are outlined in white.

The approach we adopted in attempting to discover the extent to which the observers erred and to correct for their misperception of endocardial borders was to collect three-dimensional phantom data comparable to patient studies. The phantom used was a commercially available cardiac insert phantom (Data Spectrum Corp., Chapel Hill, NC) consisting of a myocardial chamber of 115 ml which was loaded with 315 μCi ^{99m}Tc in water. No simulated defects were used. The simulated LV cavity of the phantom contained no activity, only water. Once assembled, the cardiac phantom was submerged in an elliptical tub phantom containing 4.5 liters of water and 2.8 mCi of ^{99m}Tc. The apex-to-base axis of the simulated LV was oriented at a 45° LAO position and was angled caudally 20° from the horizontal.

The phantom was acquired for 64 angles over 180° and provided 25K counts from the simulated myocardium imaged at the 40° LAO projection. This was similar to the 30K average myocardial counts of our patient data imaged in the 40° LAO projection image. The same filters were used for constructing the HLA and VLA tomograms for patient studies. Mid-ventricular HLA and VLA tomographic slices and corresponding count profiles are shown in Figure 4. Note that even though the phantom contained uniform radionuclide concentration within carefully machined plexiglass walls, count profiles demonstrate a gradual spatial transition from maximum to minimum counts, as expected for any imaging system having a point spread function of substantial width. This is shown in greater detail in Figure 5, where measured counts through the mid-ventricular HLA phantom projection are plotted against pixel location, superimposed with the actual known input radionuclide spatial distribution. These results illustrate that defining endocardial borders at the pixel locations corresponding to 34% of maximum counts will result in an underestimation of ventricular cavity dimensions.

The actual inner diameter of the cylindrical chamber of the phantom used to generate the images and curves of Figures 4 and 5 was measured by calipers to be 5.9 ± 0.1 cm. The distance between the pixels located at 34% of count maxima of the combined average of four HLA and four VLA count profiles, corre-

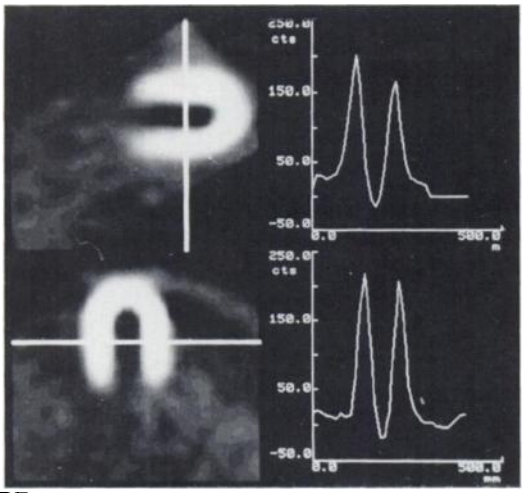

FIGURE 4. Horizontal and vertical long-axis slice count rate profiles obtained from the cardiac phantom.

sponding to the inner part of the chamber, was measured as 4.8 ± 0.3 cm. Therefore, we concluded that defining inner borders at locations corresponding to 34% of maximum HLA and VLA counts in the cylindrical phantom underestimated these dimensions by an average of 1.1 cm, or 19%. Since we had acquired and processed the phantom data as nearly identically to human data as was feasible, we proceeded on the assumption that this diameter correction should be the same for both phantom data and patient data.

Therefore, the formula to calculate LV volume from gated MIBI studies was empirically modified whereby the vertical and horizontal dimensions of each elliptical slice were each increased by a constant value of c = 1.1 cm:

$$V' = \sum_{j=1}^{N} (\pi/4) H_j' \times V_j' \times T, \qquad \text{Eq. 3}$$

where $H_j' = H_j + c$, and $V_j' = V_j + c$.

The implications of this modification, which represents an approximate scatter correction, are graphically illustrated in Figure 6, where it is seen that all dimensions are increased to form elliptical cylindrical slices expanded beyond their uncorrected borders.

The modified formula (Equation 3) to calculate LV volume was

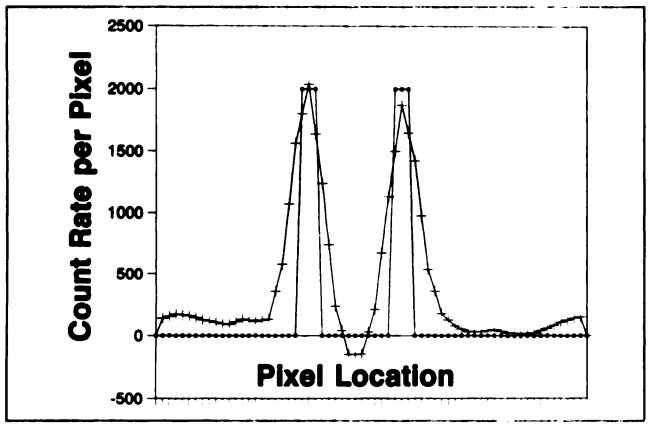

FIGURE 5. Cardiac phantom count rate profile compared to actual endocardial and epicardial phantom borders.

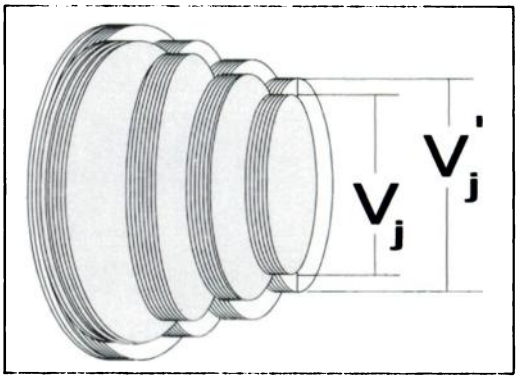

FIGURE 6. Modification of Figure 2, wherein the height V and width H are increased by a scatter correction factor c.

applied to patient studies for LV cavity tracings performed by observer 1 and both sets of tracings performed one month apart by observer 2.

Data Analysis and Statistics

By means of linear regression analysis, LVEF values determined by gated MIBI SPECT were compared to those in the same patients derived from gated equilibrium radionuclide angiocardiography. Also, intraobserver agreement was evaluated for observer 2 using linear regression analysis. Heart rates for equilibrium radionuclide angiography and gated ^{99m}Tc-sestamibi SPECT were compared using the t-test for paired data.

RESULTS

In Figure 7, the results of the three observations are plotted on the y-axis and compared to EFs calculated from equilibrium radionuclide angiocardiography studies on the x-axis. Individual determinations of correlation coefficients ranged from 0.79 to 0.88, for which the slope is 1.07 and standard error of the estimate is 7.7%.

The results of the correlation between EF determined by gated MIBI SPECT and gated blood-pool imaging for each observer are presented in Table 1. The correlation coefficient was 0.79 for observer 1 and 0.86 and 0.88 for the two measurements of observer 2, respectively. Averaging the three LVEF determinations produced correlations with gated blood-pool EFs of r = 0.93, treating all LVEF results in a combined data set of independent values resulted in an the r value of 0.83. Between observers 1 and 2, interobserver agreement was 75%. For observer 2, intraobserver agreement was 75%.

DISCUSSION

The results of this study indicate that LVEF can be estimated with reasonable accuracy and precision from gated MIBI SPECT myocardial perfusion images. This functional information for many patients may be adjunctive to the results of the perfusion scan with regard to diagnosis and prognosis. Patients in whom the assessment of resting ventricular function in addition to stress and rest perfusion imaging may be of value include patients with myocardial infarction and those with cardiomyopathy and valvular disease, which may coexist with coronary artery disease.

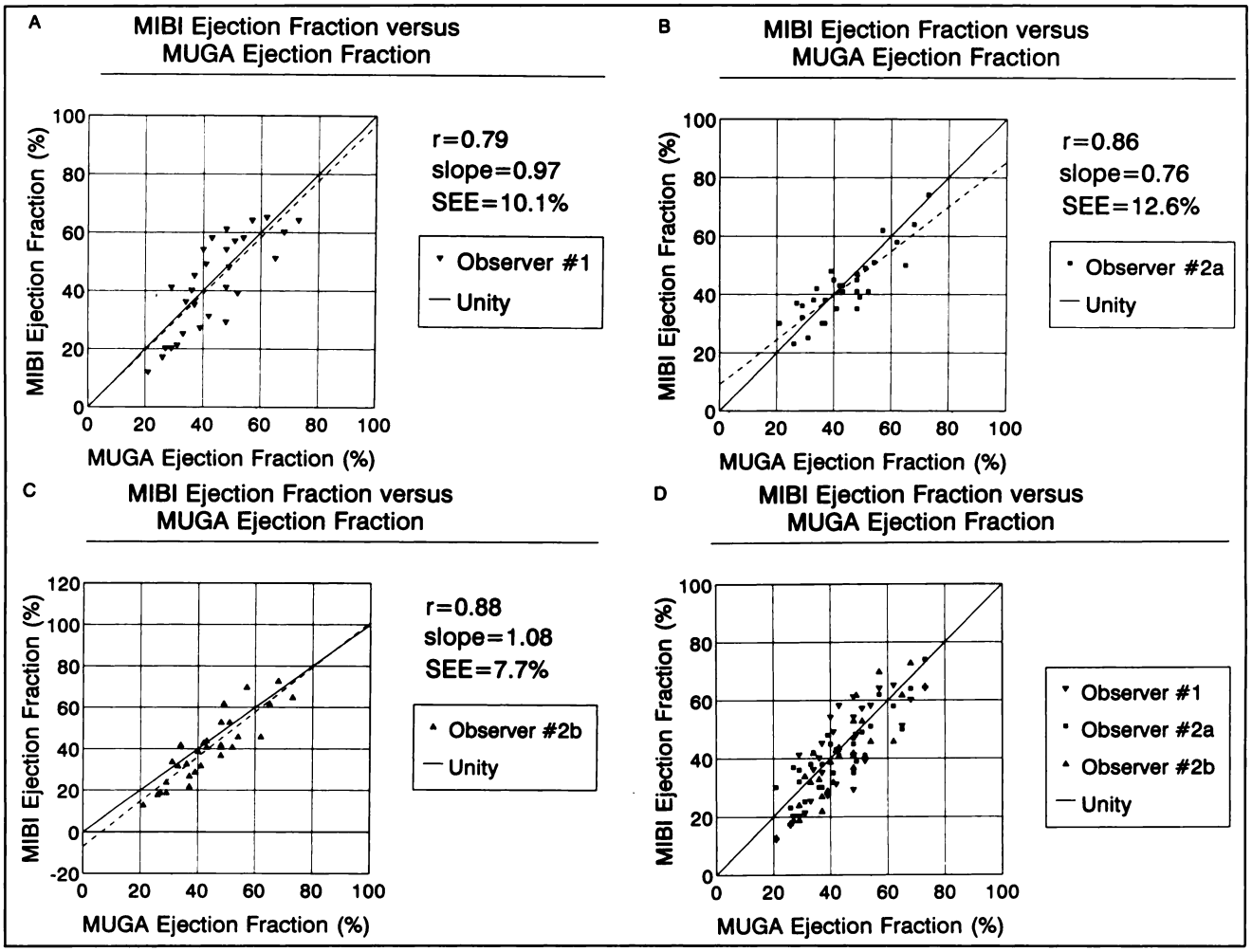

FIGURE 7. Comparison of LVEF determined from gated MIBI SPECT studies and from equilibrium radionuclide angiography (MUGA) studies in 30 patients with prior myocardial infarction. Results shown are for observer 1 (A), for the first EF determination of observer 2 (B), for the second determination by observer 2 (C) and for all EFs of both observers plotted on the same graph versus MUGA ejection fraction values (D).

Since EF is determined by means of computer analysis of data already obtained for the perfusion scan, the patient is spared the additional time and expense of either echocardiography or radionuclide ventriculography and the additional radiation exposure of the latter.

No additional acquisition time was required to perform gated SPECT as compared to a nongated study. However, computer processing time was increased because the data are gated and the additional amount of time required to obtain the gated mid-ventricular HLA or VLA images in a form suitable for viewing was 5 min. Once the HLA and VLA mid-ventricular gated data have been processed, the additional time required to preview the images, select the ED and ES frames and draw the endocardial borders was 10 min.

TABLE 1
Regression Analyses MIBI EFs Versus MUGA EFs

Comparitor	r	Intercept	Slope	s.e.e.
Observer 1	0.79	0.11	0.97	10.1
Observer 2a	0.86	9.2	0.76	12.6
Observer 2b	0.88	−7.0	1.08	7.6
Averaged	0.93	0.01	0.93	5.1
Combined	0.83	0.01	0.94	8.2

Interobserver agreement (r) = 0.75 and interobserver variability (r) = 0.75.

There are several limitations to the method of determining LVEF from gated MIBI SPECT described in this study. There is uncertainty in identification of true end-systole from eight-frame per cycle gated images. Such an inadequate sampling error would tend to result in a systematic underestimation of EF because error in estimation of end-systole would always overestimate ESV and thus underestimate EF. Second, delineation of the valve plane is an approximation and probably a significant source of interobserver and intraobserver variability. Third, there was no compensation made for rotational or translational movement of the heart during the cardiac cycle. Thus, the same region of myocardium may not always lie within a defined ROI at both end-diastole and end-systole. This error may result in underestimation of the degree of re-

gional dysfunction and a consequent overestimation of EF. Finally, the scatter correction value "c" used was the same for the entire heart, and the same correction factor was used for all patients. The distance by which to relocate detected myocardial boundaries is a function of an individual's wall thickness (*10*) and would only be constant if all patients' myocardia were the same thickness. None of these assumptions is likely to be entirely correct and would be expected to introduce error in endocardial border detection.

Since gated stress ^{99m}Tc-MIBI studies were acquired 30–60 min following treadmill or pharmacologic stress, stress-induced wall motion abnormalities theoretically could have persisted for an hour and contributed to LV dysfunction detected on the gated MIBI SPECT study, but not on the resting equilibrium radionuclide ventriculography study. However, no patient enrolled in this study demonstrated severe stress-induced ischemia, so disagreement between the two techniques to calculate EF for this reason is unlikely.

Intraobserver and interobserver reproducibility in determination of LVEF from gated MIBI SPECT were suboptimal (r = 0.75). Due to this imprecision, the technique is limited in following patients after infarction for small changes in global ventricular function. The most likely source of imprecision is the drawing of endocardial borders in patients with infarcts and associated extensive, severe perfusion defects (Fig. 1). However, in no subject was the myocardium so poorly defined, particularly using the black and white image display, that the observer was unable to estimate the endocardial border of an infarcted region. A further contribution to the subjectivity in this method is in defining the endocardial borders and valve planes, as described previously. Future software development may provide automated or semi-automated endocardial border detection and valve plane determination and could consequently increase precision (*12*). However, as of this writing, reported results of automatic endocardial edge-finding algorithms applied to gated MIBI tomograms in CAD patients for measurement of LVESV [(r = 0.87) (*12,13*)] and LVEF [(r = 0.72) (*14,15*)] are not much better than what we have observed with our manual method.

The method we have developed can be applied accurately only to gated MIBI SPECT studies acquired using the same camera/collimator system, acquisition protocol and image processing and display software described above in the Methods section, since variation in parameters such as image count density, data filtering, system spatial resolution, Compton scatter, and color display scale will influence endocardial border definition. Therefore, in order to adopt this method to other camera/computer systems, an analysis of phantom data acquired and processed in a manner similar to that described in the Methods section is recommended. Also, gated SPECT and evaluation of LVEF was performed in this study for only stress, high dose ^{99m}Tc-MIBI studies. We have had no experience with gated resting and/or low-dose studies.

In conclusion, gated ^{99m}Tc-MIBI SPECT is a method whereby myocardial perfusion and ventricular function can be evaluated simultaneously. Although this method is relatively simple and operator-friendly, care is needed to obtain reproducible results.

REFERENCES

1. Verani MS, Jeroudi MO, Mahmarian JJ, et al. Quantification of myocardial infarction during coronary occlusion and myocardial salvage after reperfusion using cardiac imaging with technetium-99m hexakis 2-methoxyisobutyl isonitrile. *J Am Coll Cardiol* 1988;12:1573–1581.
2. Gibbons RJ, Verani MS, Behrenbeck T, et al. Feasibility of tomographic ^{99m}Tc-hexakis-2-methoxy-2-methylpropyl-isonitril imaging for the assessment of myocardial area at risk and the effect of treatment in acute myocardial infarction. *Circulation* 1989;80:1277–1286.
3. Mannting F, Mannting MGM. Gated SPECT with technetium-99m-sestamibi for assessment of myocardial perfusion abnormalities. *J Nucl Med* 1993;34:601–608.
4. Grucker D, Florentz P, Ozwald T, Chambron J. Myocardial gated tomoscintigraphy with Tc-99m-methoxy-isobutyl-isonitrile (MIBI): regional and temporal activity curve analysis. *Nucl Med Commun* 1989;10:723–732.
5. Marcassa C, Marzullo P, Parodi O, Sambucetti G, L'Abbate A. A new method for noninvasive quantitation of segmental myocardial wall thickening using Tc-99m-2-methoxy-isobutyl-isonitrile: scintigraphic results in normal subjects. *J Nucl Med* 1990;31:173–177.
6. Braat SH, De Swann C, Brugada P, Wellens HJJ. Value of left ventricular ejection fraction in extensive anterior infarction to predict development of ventricular tachycardia. *Am J Cardiol* 1983;52:686–689.
7. Shah PK, Pichler M, Berman DS, Singh BN, Swan HJC. Left ventricular ejection fraction determined by radionuclide ventriculography in early stages of first transmural myocardial infarction. *Am J Cardiol* 1980;45:542–546.
8. Sanford CF, Corbett J, Nicod P, et al. Value of radionuclide ventriculography in the immediate characterization of patients with acute myocardial infarction. *Am J Cardiol* 1982;49:637–644.
9. Hoffman EJ, Huang SC, Phelps ME. Quantitation in positron emission computed tomography: I. Effects of object size. *J Comput Assist Tomogr* 1979;5:391–400.
10. Faber TL, Akers MS, Peshock RM, et al. Three-dimensional motion and perfusion quantification in gated single-photon emission computed tomograms. *J Nucl Med* 1991;32:2311–2317.
11. Galt JR, Garcia EV, Robbins WL. Effects of myocardial wall thickness of SPECT quantification. *IEEE Trans Med Imaging* 1990;9:144–150.
12. Nuyts J, Suetens P, Oosterlinck A, De Roo M, Mortelmans L. Delineation of ECT images using global constraints and dynamic programming. *IEEE Trans Med Imaging* 1991;10:489–498.
13. Schiepers C, Nuyts J, Mortelmans L, De Roo M. Determination of cardiac volumes in PET and SPECT by delineation of myocardium [Abstract]. *J Nucl Med* 1992;33:932.
14. Quaife RA, Faber TL, Corbett JR. Quantitative 3-dimensional SPECT assessments of myocardial perfusion, function and viability using stress perfusion imaging with Tc-99m sestamibi [Abstract]. *J Nucl Med* 1992;33:926.
15. Faber TL, Stokely EM, Peshock RM, Corbett JR. A model-based four dimensional left ventricular surface detector. *IEEE Trans Med Imaging* 1991;10:321–329.